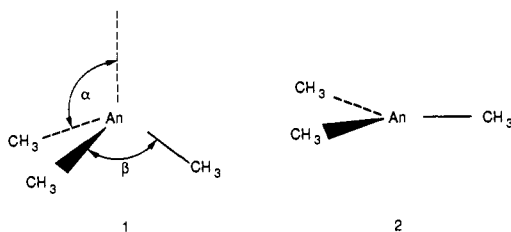


occupied orbitals and  $[5f^3]$  denotes all possible excitations of three high-spin electrons among the seven  $5f$ -like orbitals. For  $\text{NpMe}_3$  and  $\text{PuMe}_3$ , the CAS-SCF calculations involved  $5f^4$  and  $5f^5$  configurations, respectively.<sup>11</sup> For each of these three molecules there arises a dense manifold of very low-lying excited states involving  $5f^n$  configurations which span several electronvolts in energy.

For the ground electronic state of each molecule, the optimum geometry for both pyramidal (1) and planar (2)  $\text{AnMe}_3$  forms was determined,<sup>12</sup> and in each case the pyramidal structure (1) was found to be the stable form (Table I). The angle  $\alpha$  corre-



sponding to the angle between the  $\text{An}-\text{C}$  bond and the 3-fold axis was calculated to be 113.1, 111.7, and 110.2° for the series  $\text{UMe}_3$ ,  $\text{NpMe}_3$ , and  $\text{PuMe}_3$ . This is in very good accord with the known X-ray structure for  $\text{U}[\text{CH}(\text{SiMe}_3)_2]_3$ , for which  $\alpha = 111^\circ$ . The calculated  $\text{An}-\text{C}$  bond lengths decrease by 0.07 and 0.12 Å as one proceeds from U to Np to Pu. The planar structure (2) with  $C_{3h}$  symmetry in our model system corresponds to a transition state between the two equivalent pyramidal structures with  $C_3$  symmetry. The barrier along the umbrella bending mode decreases in the order 3.7 ( $\text{UMe}_3$ ), 3.3 ( $\text{NpMe}_3$ ), and 2.4 ( $\text{PuMe}_3$ ) kcal/mol, and some lengthening (0.04–0.05 Å) is noted in the bond length compared to structure 1 in each case.

The result that the pyramidal structure observed experimentally can be obtained in these model compounds indicates that the geometry does not arise from steric interactions involving bulky ligands or from lattice packing interactions. The similarity of the structures with varying  $f$ -electron count also suggests that the occupancy of  $f$  orbitals is not playing a major role. The influence of spin-orbit coupling can also be discounted as a major factor since the energies of the entire manifold of  $5f^4$  states for  $\text{NpMe}_3$ , for example, all decrease by approximately 3 kcal/mol as one proceeds along the path from planar to pyramidal geometries. While spin-orbit coupling would alter the relative ordering of states within the manifold, it would not significantly influence the overall envelope of states.

Rather, the driving force for the preference of the pyramidal structure (1) relative to the planar form (2) appears to be the involvement of  $6d$  character in the  $\text{An}-\text{C}$  bonding orbitals as a function of bending angle. This admixture occurs primarily in the  $e$  set of  $\text{U}-\text{C}$  bonding orbitals (Figure 1). For the planar structure, the  $d_{\pi}$  and  $\text{U}-\text{C}$  bonding orbitals have  $e''$  and  $e'$  symmetry, respectively, and cannot interact; as one bends, the orbitals can acquire  $d$  character in the  $C_3$  symmetry as shown in the figure. This role of  $d$  orbital participation is reflected in the increase in  $d_{xz}$  and  $d_{yz}$  populations in the Mulliken analysis from 0.04 to 0.34 electron for  $\text{UMe}_3$  as the bending angle  $\alpha$  increases from 90° to 113° while the overall  $f$  orbital population remains relatively constant along the bending path.

A more convincing demonstration of the role of  $d$  orbitals is provided by a series of calculations in which the  $d$  orbitals are deleted from the basis. For the case of  $\text{PuMe}_3$ , for example, where the calculated energy difference,  $E(\text{planar}) - E(\text{pyramidal})$ , is +2.4 kcal/mol in the full basis, this difference becomes -9.6 kcal/mol (i.e., planar lower in energy) when  $d$  functions are

removed from the calculation. Similar results were obtained for the other compounds.

**Acknowledgment.** J.V.O. thanks the Associated Western Universities for support during his visit to Los Alamos. This work has been carried out under the auspices of the U.S. Department of Energy.

### Optical Devices Based on Dye-Coated Superconductor Junctions: An Example of a Composite Molecule-Superconductor Device

Jianai Zhao, David Jurbergs, Brett Yamazi, and John T. McDevitt\*

Department of Chemistry and Biochemistry  
University of Texas at Austin  
Austin, Texas 78712-1167  
Received November 12, 1991

The use of molecular materials for the development of new and novel electronic devices has attracted much attention in the recent scientific literature.<sup>1</sup> Molecule-based devices offer prospects for enhanced sensitivity and selectivity that are not possible with conventional solid-state materials. Molecular transistors which mimic solid-state semiconductor devices have been prepared from conductive polymer, metal oxide, and redox polymer films coated on electrode surfaces.<sup>2</sup> In virtually all previous macromolecular devices, the active elements have been fabricated by organizing molecular systems onto a metal or semiconductor template surface. With the recent discovery of high-temperature superconductivity,<sup>3</sup> new opportunities exist for the development of hybrid molecule-superconductor components. In this paper, we describe methods to fabricate and demonstrate the operation of an optical sensor based on a molecular dye-coated superconductor junction.

Josephson junctions fabricated from high temperature superconductor thin films have been utilized previously to fabricate light detectors with high sensitivity ( $10^{-3}$ – $10^3$  V/W), fast response time ( $\sim$ nanosecond), and a working wavelength range from the ultraviolet to the far infrared.<sup>4</sup> The data presented in this paper will illustrate for the first time that a molecular dye can be utilized to enhance the sensitivity of these devices and provide them with wavelength selectivity (i.e., certain frequencies can be sensed more readily than others).

The composite dye-superconductor devices are fabricated according to the following steps. First,  $\sim 1000$  Å of the high-temperature superconductor  $\text{YBa}_2\text{Cu}_3\text{O}_{7-x}$  is deposited onto the surface of a clean  $\text{MgO}$  (100) substrate using the method of laser ablation.<sup>5</sup> Second, a superconductor microbridge  $\sim 3$  mm long and  $\sim 50$   $\mu\text{m}$  wide is created on the film by reapplying the laser to selective regions of the film using an imaging method similar to that previously described.<sup>6</sup> In the final step, a dye film such as octaethylporphyrin is deposited onto the microbridge by vacuum sublimation (or spin coating). A more complete description of device fabrication methods will be published in the near future.

(1) (a) Chidsey, C. E.; Murray, R. W. *Science* **1986**, *231*, 25–31. (b) Wrighton, M. S. *Science* **1986**, *231*, 32–37. (c) Smith, S. D.; Walker, A. C.; Tooley, F. A. P.; Wherrett, B. S. *Nature* **1987**, *325*, 27–31. (d) Lehn, J. M. *Angew. Chem., Int. Ed. Engl.* **1988**, *27*, 89–112. (e) Robinson, B. H.; Seeman, N. C. *Protein Eng.* **1987**, *1*, 295–300. (f) Lindsey, J. S. *New J. Chem.* **1991**, *15*, 153–180.

(2) (a) Pickup, P. G.; Murray, R. W. *J. Electrochem. Soc.* **1984**, *131*, 833–839. (b) Kittleson, G. P.; White, H. S.; Wrighton, M. S. *J. Am. Chem. Soc.* **1984**, *106*, 7389–7396. (c) Wrighton, M. S. *Comments Inorg. Chem.* **1985**, *4*, 269–294.

(3) Bednorz, J. G.; Müller, K. A. *Z. Phys. B* **1986**, *64*, 189–193. (4) (a) Enomoto, Y.; Murakami, T. *J. Appl. Phys.* **1986**, *56*, 3807–3814. (b) Kwok, H. S.; Zheng, J. P.; Ying, Q. Y. *Appl. Phys. Lett.* **1989**, *54*, 2473–2475. (c) Forrester, M. G.; Gottlieb, M.; Gavaler, J. R.; Braginski, A. I. *Appl. Phys. Lett.* **1988**, *53*, 1332–1334. (d) Enomoto, Y.; Murakami, T.; Suzuki, M. *Physica C* **1988**, *153–155*, 1592–1597.

(5) (a) Dijkkamp, D. *Appl. Phys. Lett.* **1987**, *51*, 619–621. (b) Char, K. *Appl. Phys. Lett.* **1990**, *56*, 785–787.

(6) Vase, P.; Yueqiang, S.; Freltoft, T. *Appl. Surf. Sci.* **1990**, *46*, 61–66.

(11) This results in 35 ( $S = 3/2$ ), 35 ( $S = 2$ ), and 21 ( $S = 5/2$ ) states in the CAS-SCF calculation for U, Np, and Pu, respectively.

(12) The C–H distances were held fixed at 1.09 Å assuming tetrahedral geometries. The orientation of the  $\text{CH}_3$  groups was such that the molecule had  $C_3$  symmetry for pyramidal (1) forms and  $C_{3h}$  symmetry for planar (2) forms. The angle  $\beta$  is determined from  $\alpha$  and is not a free parameter.

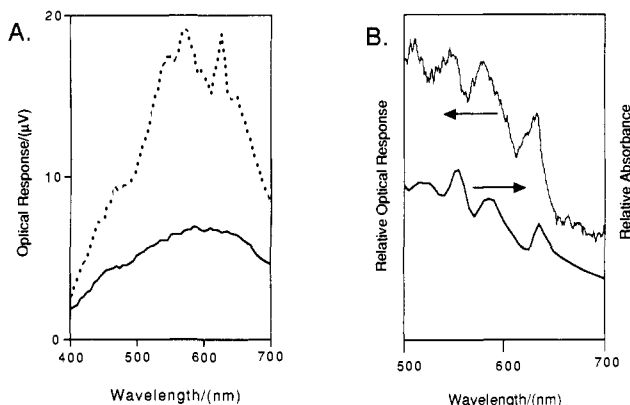


**Figure 1.** Optical response vs wavelength for a 3-mm-long  $\times$  50- $\mu$ m-wide  $\text{YBa}_2\text{Cu}_3\text{O}_{7-\delta}$  microbridge device operating at a temperature just below  $T_c$  (mid): (A) unprocessed signals for bare junction (lower curve) and junction coated with 3300 Å of octaethylporphyrin (upper curve); (B) comparison between the absorbance spectrum of an octaethylporphyrin film (1.1  $\mu$ m thick) as measured by UV-visible spectrophotometry (lower curve) and the normalized optical signal of the dye-superconductor device with the uncoated junction response subtracted (upper curve).

In order to study the optical response of the device, the thin film assembly is mounted into an optical cryostat and one voltage and one current lead are attached to either side of the microbridge. After characterization by resistivity vs temperature, current-voltage experiments, and critical current measurements, the device is cooled down to just below the transition temperature of the superconductor film and a constant direct bias current is applied across the junction. The optical response of the dye-superconductor device is measured with a lock-in amplifier as a function of wavelength by monitoring the in-phase voltage which develops across the microbridge when chopped (20–25-Hz) monochromatic light is focused onto the junction area.

The unprocessed optical response at a  $\text{YBa}_2\text{Cu}_3\text{O}_{7-\delta}$  microbridge with and without the octaethylporphyrin film is illustrated in Figure 1A.<sup>7</sup> In both cases, the largest response is recorded at around 600 nm, corresponding to the maximum throughput for the monochromator/quartz halogen light source combination. The bare junction exhibits a rather featureless response as has been described previously for similar systems.<sup>4</sup> The dye-coated superconductor structure, on the other hand, exhibits enhanced sensitivity as well as sharp features in the response curve that are absent for the bare junction. The frequencies at which enhanced responsivity occurs correspond to those wavelengths which are absorbed strongly by the dye film. Figure 1B provides a comparison between the absorption profile of the dye film and the response of the dye-superconductor microbridge. The latter has been normalized to the light intensity at a given wavelength, and the response of the uncoated junction has been subtracted. It is interesting to note that those wavelengths which are absorbed most strongly by the dye lead to the largest response for the hybrid dye-superconductor device. Thus, molecular dyes can be exploited to sensitize superconductor junctions to enhance both the responsivity<sup>8</sup> and the wavelength selectivity of the device. Moreover, since the normalized optical response of the composite device parallels the absorbance spectrum of the dye overlayer, the device can be exploited to measure the absorbance characteristics of a solid dye film.

To date we have prepared hybrid devices using dye films such as octaethylporphyrin (free base and copper), phthalocyanine, and rhodamine 6G. In all cases where degradation of the underlying superconductor was avoided, the molecular layer served to alter the response of the underlying superconductor structure in a

(7) The optical response curves were recorded at a temperature of 48 K using a bias current of 5 mA. The transition-temperature midpoint for the device was 55 K.

(8) Since there was a small increase in the microbridge resistance following the dye deposition, some of the increase in signal for the dye-coated device may be attributed to this resistance increase.

reproducible fashion. Moreover, the magnitude of the response is greatest when the device is operated near  $T_c$  and no appreciable response is observed for  $T > T_c$ .<sup>9</sup>

With the discovery of the above-described hybrid dye-superconductor devices, new opportunities arise to study energy-transfer and electron-transfer phenomena which occur between molecules and superconductors. Work is now in progress to decipher the mode of operation of the hybrid devices and to expand upon the number and types of dyes that can be exploited to sensitize superconductor junctions.

**Acknowledgment.** This work was supported by the National Science Foundation (Presidential Young Investigator Program) as well as by the Electric Power Research Institute. We thank Professor Alex de Lozanne and his research group for technical assistance related to the deposition of superconductor thin films and Professors John White and Stephen Webber for use of a laser. We also gratefully acknowledge Matthew J. Holcomb for helpful discussion and Newport Corp. for a generous equipment donation.

**Supplementary Material Available:** Description of the procedure for fabricating composite dye-superconductor devices and plots of resistivity vs temperature, current vs voltage,  $dR/dT$  vs temperature, and optical response vs temperature for  $\text{YBa}_2\text{Cu}_3\text{O}_{7-\delta}$  microbridge (7 pages). Ordering information is given on any current masthead page.

(9) The temperature response of the hybrid device parallels  $dR/dT$ , which suggests that an indirect bolometric mechanism is operative for the system described herein (see ref 4).

## New Triad Alkylation Reagent. Cross-Coupling of Indium Trialkyls with Alkenyl Halides

Ryōki Nomura,\* Shin-Ichiro Miyazaki, and Haruo Matsuda

Department of Applied Chemistry  
Faculty of Engineering, Osaka University  
Yamada-Oka, Suita, Osaka 565, Japan

Received September 17, 1991

Cross-coupling of metal alkyls with haloalkenes provides general and convenient method of preparing olefins. Among several organometallics already surveyed, organocopper reagents are the most powerful tool.<sup>1</sup> Additionally, Grignard or organozinc reagents with the assistance of transition metal catalysts have alternative values.<sup>2</sup> The scope of their power is somewhat limited to iodo- and bromoalkenes, and cross-coupling with chloroalkenes is seldom employed in practical synthetic applications. Further, the isomerization of carbanions is sometimes encountered in the cross-coupling of metal *sec*-alkyl derivatives.<sup>2a</sup> In order to get over such a limitation, aluminum alkyls and other group 13 organometallics must be applied further in the cross-coupling reactions, because they have greater tendency to form a Lewis complex with several chlorides in contrast to Grignard and organozinc reagents. Such complexation perhaps contributes to the activation of the chloride, promising a higher reactivity toward alkenyl chlorides without any isomerization through a dissociative cross-coupling manner.<sup>4</sup>

(1) For reviews, see: (a) Posner, G. H. *Org. React. (N.Y.)* **1975**, *22*, 253. (b) Worm, A. T.; Brewster, J. H. *J. Org. Chem.* **1970**, *35*, 1715.

(2) For reviews, see: (a) Kumada, M. *Pure Appl. Chem.* **1980**, *52*, 669. (b) Negishi, E. *Acc. Chem. Res.* **1982**, *15*, 340. (c) Negishi, E. *Organometallics in Organic Synthesis*; John Wiley & Sons: New York, 1980; Vol. 1, p 116. (d) Jolly, P. W. In *Comprehensive Organometallic Chemistry*; Wilkinson, G., Stone, F. G. A., Abel, E. W., Eds.; Pergamon Press: Oxford, 1982; Vol. 8, p 713. (e) Heck, R. F. *Palladium Reagents in Organic Syntheses*; Academic Press: London, 1985.

(3) Mole, T.; Jeffrey, E. A. *Organooaluminum Compounds*; Elsevier: Amsterdam, 1972; p 111.